Solitonic dynamics of ultrashort pulses in a highly nonlinear photonic-crystal fiber visualized by spectral interferometry

D. A. Sidorov-Biryukov,[1,2] A. Fernandez,[1] L. Zhu,[1] A. Verhoef,[1] P. Dombi,[1] A. Pugzlys,[1] E. E. Serebryannikov,[2] A. M. Zheltikov,[2,*] J. C. Knight,[3] and A. Baltuška[1]

[1]*Institute of Photonics, Vienna University of Technology, Vienna, Austria*
[2]*Department of Physics, International Laser Center, M. V. Lomonosov Moscow State University, Moscow, Russia*
[3]*Department of Physics, Centre for Photonics and Photonic Materials, University of Bath, United Kingdom*
**Corresponding author: zheltikov@phys.msu.ru*

Received September 12, 2007; revised October 31, 2007; accepted November 22, 2007;
posted January 10, 2008 (Doc. ID 87451); published February 22, 2008

A linear technique of phase measurement based on spectral interferometry is employed to visualize the fine details in the spectral phase of a soliton produced in a highly nonlinear photonic crystal fiber (PCF) with a resolution better than 0.1 nm. Gigahertz features have been resolved in the spectral phase of the soliton PCF output, allowing the accuracy of time-domain soliton envelope reconstruction to be improved on the timescale of a few femtoseconds. © 2008 Optical Society of America

OCIS codes: 190.4370, 190.7110.

Photonic-crystal fibers (PCFs) [1,2] suggest a remarkable flexibility and unique precision in controlling nonlinear-optical transformations of laser pulses through a careful fiber structure engineering. Such fibers have been shown to allow the generation of multioctave supercontinuum radiation [3] and efficient tunable-frequency conversion [4]. Because of the high nonlinearity of PCFs, spectral and temporal transformations of ultrashort pulses occur on a much shorter spatial scale compared with pulse evolution in a standard fiber. High-order dispersion effects, on the other hand, lead to the generation of transient field waveforms with complicated temporal envelopes, spectra, and chirps. Development of adequate techniques for an accurate measurement of these parameters would give the key to understanding the details of pulse-transformation dynamics necessary for the creation of advanced optical components based on the currently available highly nonlinear fiber, such as PCFs and fibers made of high-n_2 materials. Cross-correlation frequency-resolved optical gating (XFROG) [5] has been intensely used over the past few years to reconstruct the temporal envelope, spectrum, and spectral phase of laser pulses transmitted through PCFs [6]. This technique is ideally suited for providing panoramic survey spectrograms, revealing the frequency- and time-domain structure of broadband PCF output, which is of special value for PCF-based supercontinuum sources. Although short solitonic features in PCF output can be readily made visible by the XFROG technique [7], the fine structure of these features often remains unresolved, as the spectral resolution of XFROG is intrinsically limited by the nonlinear nature of the sum-frequency-generation process involved in XFROG-trace generation and the use of short reference pulses.

Here we demonstrate that a linear technique of phase measurement based on spectral interferometry (SI) [8] enables a full high-resolution reconstruction of an optical field in a light pulse undergoing nonlinear transformations in a highly nonlinear PCF. With this method, gigahertz-scale variations have been resolved in the spectral phase of the soliton PCF output, enabling an accurate reconstruction of the time-domain soliton envelope.

In experiments, we studied the soliton dynamics of light pulses produced by a ytterbium diode-pumped solid-state laser (Yb DPSSL) oscillator in a silica–air highly nonlinear PCF (Fig. 1). Based on second-harmonic-generation frequency-resolved optical gating measurements, the pulse width of the ytterbium laser output was estimated as 50 fs [inset 1 in Fig. 2(a)] with the spectrum of laser pulses centered

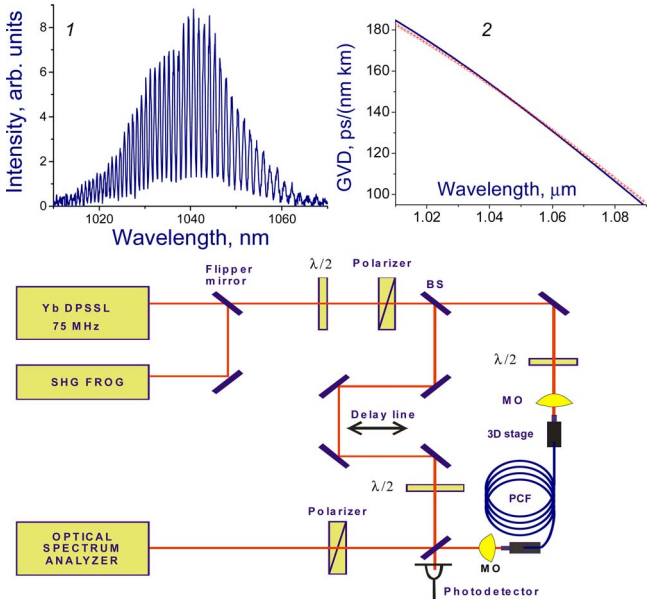

Fig. 1. (Color online) Diagram of the experimental setup. Yb DPSSL, ytterbium diode-pumped solid-state laser; λ/2, half-wave plates; MO, micro-objectives; BS, beam splitter; PCF, photonic-crystal fiber. The insets show (1) a typical interferogram recorded with a 50 fs Yb DPSSL output and (2) the wavelength dependence of the group-velocity dispersion (GVD) of the PCF reconstructed from SI measurements (solid line) and calculated using the localized function technique (dashed line).

around 1040 nm [inset 2 in Fig. 2(a)]. The pulse repetition rate was equal to 75 MHz, and the peak power of the laser pulses was varied in our experiments from 1 to 80 kW. The laser output was divided into two beams with a beam splitter. The first of these beams served as a probe field, which was launched into a highly nonlinear PCF placed in one arm of a Mach–Zehnder interferometer (Fig. 1). The second beam, transmitted through a tunable delay line in the second arm of the interferometer, provided a reference signal for the measurement of an interferogram [8] $S(\omega)=I_{PCF}(\omega)+I_{ref}(\omega)+2[I_{PCF}(\omega)I_{ref}(\omega)]^{1/2}\times\cos[\varphi(\omega)+\omega\tau]$, where I_{PCF} and I_{ref} are the spectral intensities of the PCF output and the reference field, $\varphi=\varphi_{PCF}+\varphi_{nl}$ is the phase that the probe field acquires in the PCF owing to the phase shift φ_{PCF} induced by the linear fiber dispersion and the nonlinear phase shift φ_{nl}, ω is the radiation frequency, and τ is the tunable delay time of the reference pulse.

In the regime of low-peak powers, when $\varphi_{nl}\ll\varphi_{PCF}$, SI interferograms are insensitive to the specific spectral phase profile $\varphi_0(\omega)$ of the reference field, as SI measures the phase of the PCF output, given by $\varphi_{PCF}(\omega)+\varphi_0(\omega)$ for low-peak powers, relative to the phase of the reference field, $\varphi=(\varphi_{PCF}+\varphi_0)-\varphi_0=\varphi_{PCF}$. Spectral interferograms $S(\omega)$ measured with a resolution better than 0.1 nm (inset 1 in Fig. 1) were employed to extract the spectral phase $\varphi(\omega)$ of the probe field at the output of PCF by using a standard SI phase-retrieval algorithm [9]. The temporal envelope of the PCF output was then calculated by taking the Fourier transform of the spectrum measured at the output of the fiber with the spectral phase $\varphi(\omega)$ defined from SI measurements.

For a test experiment, the Yb DPSSL output was stretched in a 59 cm block of SF57 glass to a pulse width of ~3.1 ps. With such a pulse width, the input peak power launched into the PCF was too low to induce any spectral broadening, $\varphi_{nl}\approx 0$, allowing the linear PCF dispersion profile to be readily reconstructed from SI measurements. With the PCF dispersion profile (and, hence, the linear phase shift φ_{PCF}) reconstructed from one of the low-input-peak-power SI measurements, the phase difference $\Delta\varphi=\varphi-\varphi_{PCF}$ was found to be close to zero everywhere within the studied wavelength range, exhibiting only a weak dependence on the pulse peak power at least for input peak powers below 30 W. PCF dispersion profiles extracted from SI measurements, as shown in inset 2 to Fig. 1, agree very well with the results of calculations performed by using the localized function method [10].

In experiments where the femtosecond Yb DPSSL output was directly launched to the PCF without a stretching stage, the above-described procedure of PCF dispersion reconstruction worked well only for input peak powers below 50 W. Above this level, nonlinear effects start to play a noticeable role in pulse-propagation dynamics. For a PCF with a 2 μm diameter core, a light pulse with an initial central wavelength of 1040 nm senses anomalous dispersion, tending to evolve toward a soliton above a certain level of peak powers (Figs. 2 and 3). Thus, whereas for input peak powers well below 50 W, the fiber dispersion lengthened the pulse up to ≈500 fs within a 30 cm section of PCF, for input peak powers above 50 W, dispersion-induced pulse spreading was suppressed, leading to a progressive shortening of the PCF output pulse with the growth in the input peak power [Fig. 2(a)], accompanied by a narrowing of the central lobe and a buildup of noticeable sidelobes in the PCF output spectrum [Fig. 2(b)]. For a PCF output pulse with an energy of 70 pJ, the pulse width was estimated as 130 fs (the inset to Fig. 3).

To model pulse-propagation dynamics observed in experiment, we simulated the evolution of a short-pulse envelope using the generalized nonlinear Schrödinger equation (GNSE) [11] for the field envelope $A=A(z,t)$: $\frac{\partial A}{\partial\xi}=i\Sigma_{k=2}^{6}\frac{(i)^k}{k!}\beta^{(k)}\frac{\partial^k A}{\partial\tau^k}+P_{nl}(\xi,\tau)$, where z is

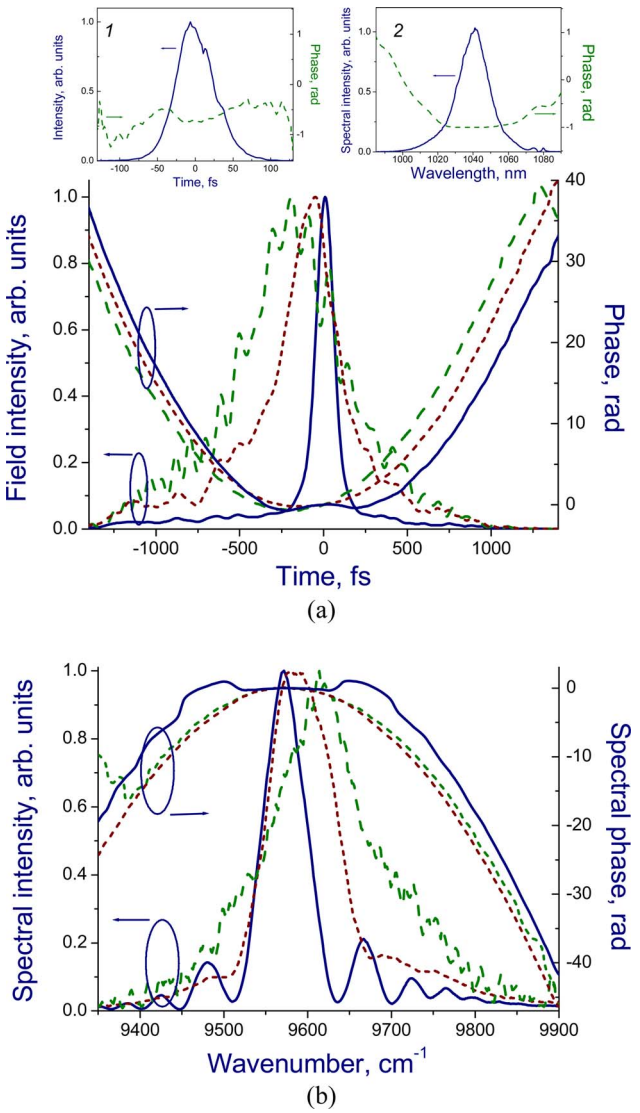

Fig. 2. (Color online) Temporal envelope with the chirp (a) and the spectrum with the spectral phase (b) for a laser pulse transmitted through a 30 cm PCF. The input pulse width is about 50 fs. The input peak power is 4 kW (dashed curve), 50 kW (dotted curve), and 75 kW (solid curve). The insets show (1) the temporal envelope and the chirp and (2) the spectrum and the spectral phase of the input pulse.

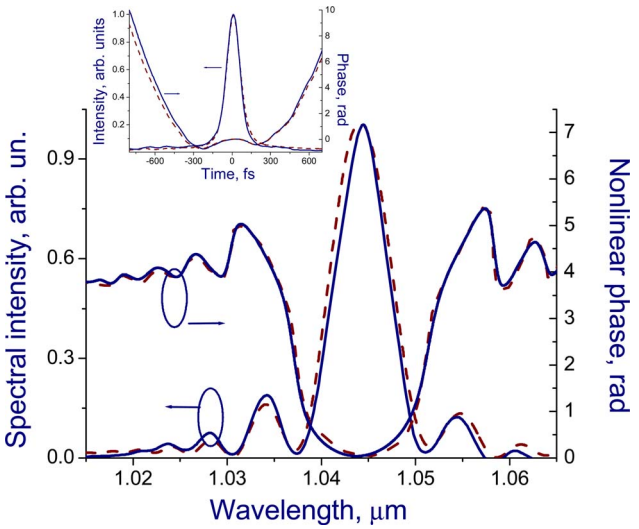

Fig. 3. (Color online) Spectrum and the nonlinear spectral phase $\varphi_{nl}=\varphi-\varphi_{PCF}$ of the PCF output extracted from SI measurements (solid curves) and simulated by solving the GNSE (dashed curves). The inset shows the temporal envelope and the chirp of the PCF output defined through the Fourier transform of the SI data (solid curve) and simulated by numerically solving the GNSE equation (dashed curve). The fiber length is 30 cm, and the laser pulse energy is 70 pJ.

the propagation coordinate, t is the time variable, τ is the retarded time, $\beta^{(k)}=\partial^k\beta/\partial\omega^k$ are the coefficients in the Taylor-series expansion of the propagation constant β, $P_{nl}(\xi,\tau)=i\hat{F}^{-1}[n_2\omega c^{-1}S_{eff}^{-1}\tilde{p}_{nl}(\xi,\omega_0-\omega)]$ is the nonlinear polarization, n_2 is the nonlinear refractive index of the fiber material, ω is the current frequency, ω_0 is the central frequency of the input field, c is the speed of light, S_{eff} is the frequency-dependent effective mode area, the operator $\hat{F}^{-1}(\bullet)$ denotes the inverse Fourier transform, $\tilde{p}_{nl}(\xi,\omega-\omega_0)=\hat{F}[A(\xi,\tau)\int_{-\infty}^{\infty}R(t)|A(\xi,\tau-t)|^2\mathrm{d}t]$ is the frequency-domain nonlinear polarization, $\hat{F}(\bullet)$ is the Fourier transform operator, and $R(t)$ is the Raman response function.

Within the entire studied range of input peak powers, the GNSE-based simulations provide an ideal fit for the measured spectra, spectral phase, temporal envelope, and chirp at the output of the fiber (Fig. 3). The significance of a high spectral resolution provided by the SI phase measurement technique is illustrated by Fig. 3, where both SI measurements (solid curve) and GNSE-based simulations (dashed curve) reveal an oscillatory behavior of the nonlinear part of the spectral phase φ_{nl} in the tails of the spectrum. With a typical oscillation period of these phase variations estimated as 6 nm for the experimental conditions of Fig. 3, their oscillation frequency is about 20 GHz. In numerical simulations, these oscillations of the spectral phase were completely suppressed when the pulse peak power was chosen in such a way as to achieve an exact balance between dispersion and nonlinearity. This finding suggests that the detected ripples of the spectral phase are induced by a mismatch between the input pulse parameters and parameters of a soliton arising as a result of pulse-propagation dynamics in the PCF. Fourier transform of the experimental spectral data with an artificial suppression of the gigahertz ripples in computations yielded a 25 fs error in the reconstruction of a temporal pulse envelope. This result illustrates how a high spectral resolution of the implemented SI phase-measurement technique translates into a few-femtosecond precision of field envelope reconstruction in the time domain.

We have thus presented high-resolution spectral phase measurements on the soliton output of a highly nonlinear PCF using a linear SI technique. In the regime of low-input peak powers, when the nonlinear phase shifts are negligible, the SI phase-measurement technique is shown to be ideally suited for a precise reconstruction of PCF dispersion profiles. For high pulse peak powers, an SI-based dispersion-measurement technique is limited by the buildup of the nonlinear phase, which complicates dispersion reconstruction from SI. In this latter regime, however, SI offers several important advantages over XFROG as a method for a phase characterization of light fields transformed by highly nonlinear systems. These include a high spectral resolution of phase measurements (better than 0.1 nm in our experiments) and the linear nature of measurements, involving no nonlinear-optical operations on light fields.

We are grateful to F. Krausz, A. Galvanauskas, and A. B. Fedotov for the support of this work and valuable discussions. This study was supported in part by the Austrian Science Fund (grants SFB-16 “ADLIS” and U33 N16), equipment loan from Max Planck Institut für Quantenoptik, Garching, the Russian Foundation for Basic Research.

References

1. P. St. J. Russell, Science **299**, 358 (2003).
2. J. C. Knight, Nature **424**, 847 (2003).
3. J. K. Ranka, R. S. Windeler, and A. J. Stentz, Opt. Lett. **25**, 25 (2000).
4. D. A. Akimov, E. E. Serebryannikov, A. M. Zheltikov, M. Schmitt, R. Maksimenka, W. Kiefer, K. V. Dukel’skii, V. S. Shevandin, and Yu. N. Kondrat’ev, Opt. Lett. **28**, 1948 (2003).
5. S. Linden, J. Kuhl, and H. Giessen, Opt. Lett. **24**, 569 (1999).
6. X. Gu, L. Xu, M. Kimmel, E. Zeek, P. O’Shea, A. P. Shreenath, R. Trebino, and R. S. Windeler, Opt. Lett. **27**, 1174 (2002).
7. S. O. Konorov, D. A. Akimov, A. A. Ivanov, E. E. Serebryannikov, M. V. Alfimov, K. V. Dukel’skii, A. V. Khokhlov, V. S. Shevandin, Yu. N. Kondrat’ev, and A. M. Zheltikov, Appl. Phys. B **79**, 289 (2004).
8. L. Lepetit, G. Cheriaux, and M. Joffre, J. Opt. Soc. Am. B **12**, 2467 (1995).
9. M. Takeda, H. Ina, and S. Kobayashi, J. Opt. Soc. Am. B **72**, 156 (1982).
10. T. M. Monro, D. J. Richardson, N. G. R. Broderick, and P. J. Bennet, J. Lightwave Technol. **18**, 50 (2000).
11. G. P. Agrawal, *Nonlinear Fiber Optics* (Academic, 2001).